(TiAlSi)N中熵涂层的微观组织与力学性能研究

张亚南，张　豪，周子超，肖宇琦，邓　娜，付彬芸，多树旺
(江西科技师范大学材料与机电学院 江西省材料表面工程重点实验室，江西 南昌 330013)

[摘　要] 为提升机械零件表面涂层的防护效用,结合中熵合金的独特设计理念,采用等离子体增强磁控溅射(PEMS)技术在316L不锈钢表面沉积(TiAlSi)N涂层。使用X射线能谱仪(EDS)、X射线衍射仪(XRD)、场发射扫描电子显微镜(FE-SEM)和原子力显微镜(AFM)分析涂层的化学成分、晶体结构、微观形貌和表面粗糙度。使用纳米划痕/压痕仪测试涂层的结合强度、硬度和弹性模量。EDS分析结果表明(TiAlSi)N为中熵陶瓷涂层。(TiAlSi)N涂层为非晶态,涂层表面平整致密,并且具有良好的力学性能,其结合强度、硬度和弹性模量分别约为25 N、21 GPa和225 GPa。试验结果可为未来深入研究该类涂层体系提供有价值的数据参考。

[关键词] 等离子体增强磁控溅射；中熵合金；(TiAlSi)N涂层；微观结构；纳米压痕
[中图分类号] TG174.44　　[文献标识码] A　　doi：10.16577/j.issn.1001-1560.2022.0062
[文章编号] 1001-1560(2022)03-0023-05

Microstructure and Mechanical Properties of (TiAlSi)N Medium Entropy Coatings

ZHANG Ya-nan, ZHANG Hao, ZHOU Zi-chao, XIAO Yu-qi, DENG Na, FU Bin-yun, DUO Shu-wang
(Jiangxi Key Laboratory of Surface Engineering, School of Materials and Mechanical & Electrical Engineering, Jiangxi Science and Technology Normal University, Nanchang 330013, China)

Abstract: In order to improve the protective effect of the surface coating of mechanical parts, combining with the unique design concept of medium entropy alloy, (TiAlSi)N coatings were deposited on surface of 316L stainless steel by plasma enhanced magnetron sputtering (PEMS). The chemical composition, crystal structure, micro-morphology and surface roughness of coatings were analyzed using X-ray energy dispersive spectrometer (EDS), X-ray diffractometer (XRD), field emission scanning electron microscope (FE-SEM) and atomic force microscope (AFM). The bonding strength, hardness and elastic modulus of the coatings were tested with nano scratch / indentation instrument. EDS analysis results showed that (TiAlSi)N coating was a medium entropy ceramic coating. (TiAlSi)N coatings possessed an amorphous structure, a smooth and compact surface, and good mechanical properties. The bonding strength, hardness and elastic modulus were 25 N, 21 GPa and 225 GPa, respectively. These experimental results would provide a valuable data reference for further future research on this kind of coating systems.

Key words: PEMS; medium entropy alloy; (TiAlSi)N coating; microstructure; nanoindentation

0　前　言

(TiAlSi)N纳米复合涂层具有高硬度、强附着力、低摩擦系数及优异的抗高温氧化性能[1-6],成为国内外的研究热点,并且已经在工业领域得到了广泛应用。该涂层通常为非晶态Si_3N_4包裹着结晶态(Ti, Al)N的复合结构(nc-TiAlN/a-Si_3N_4),该结构使(TiAlSi)N涂层具有卓越的力学性能和热学性能[1, 7-12]。随着科技的发展和工业的进步,开发综合性能更加优异的涂层材料是当务之急[13]。

中熵合金是近年来在非晶合金和高熵合金的基础上开发的一种具有广阔应用前景的新型合金。同高熵合金类似,通过适当的组元设计,中熵合金可以获得诸多优异性能,如强热稳定性、高硬度、耐磨耐蚀、抗高温氧化等[14-20]。此外,与高熵合金相比,中熵合金具有组分简单、成分易控等优点,这表明将"中熵"引入新型智能涂层设计具有一定的可行性。

常用的涂层制备技术有电弧离子镀、离子束、磁控

[收稿日期] 2021-09-28
[基金项目] 江西省井冈学者奖励计划;国家自然科学基金(51865015);江西省教育厅科技计划项目(GJJ190607, GJJ180596);江西科技师范大学本科生科研项目(20201404091);江西科技师范大学博士科研启动基金(2020BSQD011)资助
[通信作者] 张　豪(1986-),副教授,主要研究方向为陶瓷涂层与薄膜材料,E-mail:zhangyinghao1985@126.com;
多树旺(1975-),教授,主要研究方向为PVD硬质涂层的制备与应用,E-mail:swduo@126.com

溅射等，其中磁控溅射技术具有沉积范围广、靶材种类多、涂层纯度高、膜基结合牢及成分易控制等优点，在工业领域得到广泛应用[21-24]。然而，传统磁控溅射技术金属离化率低，溅射粒子多以原子态存在，涂层综合性能不佳。等离子体增强磁控溅射(Plasma Enhanced Magnetron Sputtering，PEMS)技术在传统磁控溅射系统的基础上引入热钨丝作为电子发射源[25]，能够提高金属离化率及涂层沉积效率，采用PEMS技术可望提升现有涂层的综合性能。鉴于此，结合本课题前期研究，本工作通过多靶共溅射方式，采用PEMS技术在316L不锈钢表面沉积(TiAlSi)N中熵陶瓷涂层，并详细研究了涂层的化学成分、微观组织、晶体结构、结合强度、显微硬度等性能。

1 试验

使用MS650B型回旋式磁控溅射系统在尺寸15 mm×10 mm×2 mm的316L不锈钢表面沉积(TiAlSi)N涂层。选用纯度为99.99%的Al靶、Si靶和纯度为99.7%的Ti靶作为镀膜材料(规格416 mm×106 mm×12 mm)。溅射气体为高纯氩气，反应气体为高纯氮气。首先对基体材料磨抛和丙酮、乙醇超声清洗，并吹干装炉。为进一步去除基体表面污染物，在Ar气氛下，当本底真空优于3×10^{-3} Pa时，偏压清洗基体30 min。此外，Ar^+轰击还可活化基体表面，有利于后续制备涂层与基体的良好结合。为减缓应力影响，进一步增强涂层与基体间的附着力，沉积(TiAlSi)N涂层前，先在基体表面预沉积Ti结合层和TiN过渡层。(TiAlSi)N涂层制备工艺参数如下：本底气压3×10^{-3} Pa，工作气压0.5 Pa，沉积温度300 ℃，基体偏压-50 V，氮气流量40 mL/min，氩气流量60 mL/min，沉积时间180 min，钛靶功率1 000 W，硅靶功率250 W，铝靶功率125 W。

采用INCA X射线能谱仪(EDS)分析涂层的化学组成。采用XRD-6100 X射线衍射仪(XRD)分析涂层的晶体结构，扫描速度为2 (°)/min。为减弱基体的影响，采用D8 ADVANCE掠入射XRD进一步分析(TiAlSi)N涂层的晶体结构，掠入射角为0.5°。采用SIGMA场发射扫描电子显微镜(FE-SEM)观察涂层的表、截面形貌。采用CSPM5500原子力显微镜(AFM)在轻敲模式下记录涂层的三维形貌及表面粗糙度。采用NANOVEA PB1000微纳米力学测试系统测试涂层的结合强度、硬度和弹性模量。

2 结果与讨论

2.1 涂层的化学组成

EDS测试结果显示，(TiAlSi)N涂层中Ti，Al，Si，N元素的原子分数依次为18.6%，16.3%，14.7%，50.4%。显然，涂层中合金元素和氮元素相对原子含量比约为1∶1，且各合金元素的原子含量比也接近于等摩尔比。基于Boltzmanm理论，N种元素以等摩尔比形成合金，其构型熵ΔS_{conf}可以根据式(1)来计算[26]：

$$\Delta S_{conf}=-k\ln W=R\left(\frac{1}{N}\ln N+\frac{1}{N}\ln N+\cdots\cdots+\frac{1}{N}\ln N\right)=R\ln N \quad (1)$$

式中，k为玻尔兹曼常数；W为体系混乱度；R为摩尔气体常数，8.314 J/(mol·K)。本研究中，涂层的构型熵为$1.1R$，介于$1.0R\sim1.5R$之间，说明采用PEMS技术成功制备了(TiAlSi)N中熵涂层。

2.2 涂层的显微形貌

图1展示了(TiAlSi)N中熵涂层的微观形貌。

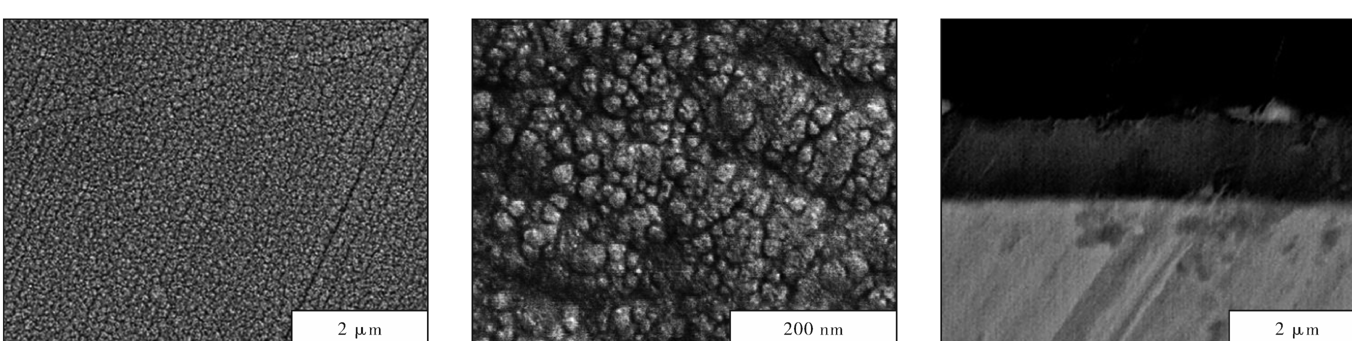

(a) 表面形貌，5 000× (b) 表面形貌，80 000× (c) 截面形貌，4 000×

图1 (TiAlSi)N中熵涂层的显微形貌

Fig. 1 Morphologies of (TiAlSi)N medium entropy coating

从涂层的低倍率表面形貌中可以看出涂层表面平整致密，并且在涂层表面观察到基体磨抛时留下的犁痕。高倍率SEM照片表明涂层呈纳米结构，涂层表面颗粒尺寸均为纳米级，未观察到明显的裂纹、孔洞等缺

陷。这可能与涂层中含有 Si 元素及中熵涂层中具有相对较高的混合熵有关[27, 28]。从涂层的截面形貌可以看到涂层总厚度约为 1.5 μm,厚度均匀,与基体结合良好。由于 Ti 结合层及 TiN 过渡层很薄,未观察到清晰的层界。

为了进一步研究(TiAlSi)N 涂层的显微结构,采用 AFM 在轻敲模式下分析了涂层的三维形貌及表面粗糙度,如图 2 所示。从图中可以看出,(TiAlSi)N 涂层表面光滑平整,晶粒细小,这与 SEM 观察结果基本吻合,其表面平均粗糙度仅为 6.53 nm。

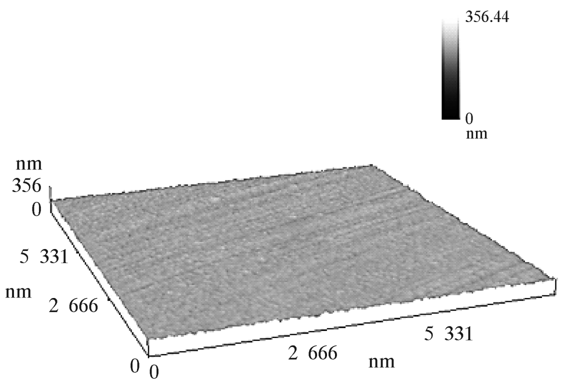

图 2　(TiAlSi)N 涂层的三维表面形貌

Fig. 2　3D surface morphology of (TiAlSi)N coating

2.3　涂层的晶体结构

图 3 给出了(TiAlSi)N 涂层的 XRD 谱。由图可以看出涂层的衍射花样主要由 1 个宽化的馒头峰和若干个强基体峰组成。涂层较薄(~1.5 μm),因此在涂层的衍射花样中检测到非常强的基体衍射峰。宽化的馒头峰表明(TiAlSi)N 涂层为非晶态结构。为了验证(TiAlSi)N 涂层的晶体结构,采用掠入射 XRD 进一步分析了(TiAlSi)N涂层的衍射花样。掠入射法减弱了基体影响,但涂层的衍射花样仍为馒头峰。为了进一步检验(TiAlSi)N 涂层为非晶结构的论断,将(TiAlSi)N

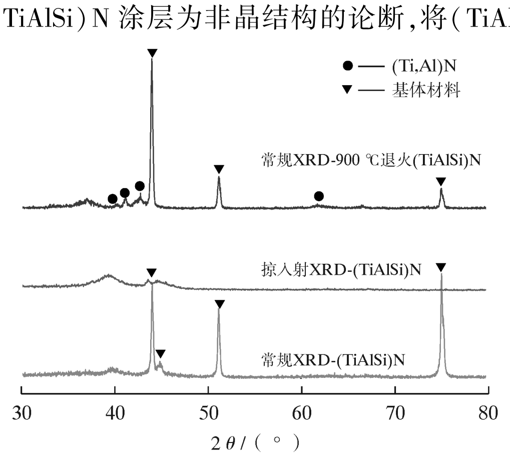

图 3　(TiAlSi)N 涂层的 XRD 谱

Fig. 3　XRD patterns of (TiAlSi)N coating

涂层在 900 ℃的真空环境中恒温处理 12 h,然后分析其 XRD 谱。经过真空热处理之后的(TiAlSi)N 涂层 XRD 谱中除了馒头峰和基体峰外,还观察到一些较弱的(Ti, Al)N 衍射峰,这进一步佐证了本研究中获得的(TiAlSi)N 涂层为非晶态。此外,在所有的 XRD 谱中均没有发现 Si 及其化合物的衍射峰,说明 Si 以非晶形式存在于涂层中。Si 的加入抑制了(Ti, Al)N 生长,涂层晶粒细化或呈现无定形态[28]。

2.4　涂层的力学性能

涂层与基体之间的结合强度是决定涂层可靠性及其使用寿命的关键指标之一。较高的结合强度可以有效防止涂层剥落,延长其服役寿命。采用划痕法测试(TiAlSi)N 涂层与基体之间的结合性能,金刚石压头划透涂层并使之从基体表面连续剥离时的最小载荷即为膜基结合失效的临界载荷[29]。划痕测试结果如图 4 所示。载荷连续变化,当载荷约为 17 N 时,涂层表面开始出现点状剥落;当载荷约为 21 N 时,点状剥落面积增大。随着载荷逐渐增大至接近 25 N 时,涂层失效由点状剥落转为连续剥落,大块基体裸露出来(图 4 中亮白色物质)。基于划痕测试原理,可以得出(TiAlSi)N 涂层的结合强度约为 25 N。

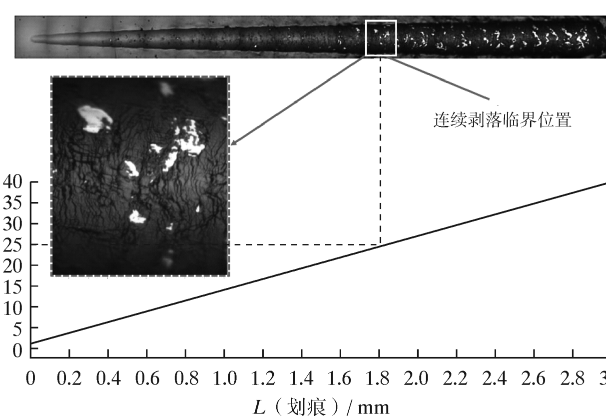

图 4　(TiAlSi)N 涂层划痕测试结果

Fig. 4　Scratch test result of (TiAlSi)N coating

硬度是材料抵抗外来物造成的穿透、变形、刮擦和侵蚀性能的关键指标。弹性模量决定了涂层的应变容限能力,而应变容限与涂层中残余热应力紧密相关。因此,硬度和弹性模量也是反映涂层可靠性的重要指标。采用压痕法在涂层表面随机选取 9 个区域测试涂层的硬度及弹性模量,然后求取平均值。结果显示,(TiAlSi)N 涂层具有相对较高的表面硬度(21 GPa)和弹性模量(225 GPa)。结合涂层形貌及晶体结构分析结果可知,涂层表面颗粒细小,涂层平整致密,并且 Si 的加入有可能在涂层中形成 Si_3N_4非晶相,其细晶强化

作用机制会进一步提高涂层的硬度及弹性模量[25]，因此(TiAlSi)N 涂层展示出较高的硬度和较大的弹性模量。

3 结 论

采用等离子体增强磁控溅射技术制备了(TiAlSi)N 中熵陶瓷涂层。涂层呈非晶态，涂层表面光滑平整，颗粒尺寸细小且排列紧密，表面粗糙度较低。纳米压痕/划痕测试结果表明涂层具有优良的综合力学性能。该工艺操作简便，组分易控，发展中熵合金涂层技术在工业领域具有潜在的应用前景。

[参 考 文 献]

[1] CHRISTIANSEN S, ALBRECHT M, STRUNK H P, et al. Microstructure of novel superhard nanocrystalline amorphous composites as analyzed by high resolution transmission electron microscopy[J]. Journal of Vacuum Science Technology B, 1998, 16(1): 19-22.

[2] PFEILER M, ZECHNER J, PENOY M, et al. Improved oxidation resistance of TiAlN coatings by doping with Si or B [J]. Surface and Coating Technology, 2009, 203(20/21): 3 104-3 110.

[3] DU H, ZHAO H B, XIONG J, et al. Effect of interlayers on the structure and properties of TiAlSiN coatings deposited on high-speed steel substrate[J]. Advanced Materials Research, 2014, 842: 302-306.

[4] HE N, LI H X, JI L, et al. High temperature tribological properties of TiAlSiN coatings produced by hybrid PVD technology[J]. Tribology International, 2016, 98: 133-143.

[5] XIAO B, LIU J, LIU F, et al. Effects of microstructure evolution on the oxidation behavior and high-temperature tribological properties of AlCrN/TiAlSiN multilayer coatings[J]. Ceramics International, 2018, 44(18): 23 150-23 161.

[6] QI B Y, HUI B H, HUA Y L, et al. Research on friction characteristics of AlCrN and TiAlSiN coatings and properties of coated tools[J]. International Journal of Precision Engineering and Manufacturing, 2019, 20(9): 1 581-1 589.

[7] VEPREK S. New development in superhard coatings: the superhard nanocrystalline-amorphous composites[J]. Thin Solid Films, 1998, 317(1/2): 449-454.

[8] CARVALHO S, REBOUTA L, CAVALEIRO A, et al. Microstructure and mechanical properties of nanocomposite (Ti, Si, Al)N coatings[J]. Thin Solid Films, 2001, 398-399: 391-396.

[9] VENNEMANN A, STOCK H R, KOHLSCHEEN J, et al. Oxidation resistance of titanium-aluminium-silicon nitride coatings[J]. Surface and Coatings Technology, 2003(174/175): 408-415.

[10] YU D, WANG C, CHENG X, et al. Microstructure and properties of TiAlSiN coatings prepared by hybrid PVD technology[J]. Thin Solid Films, 2009, 517(17): 4 950-4 955.

[11] CHANG J F, YUAN F J, SHUI L H, et al. The effects of Ag addition on the microstructure and mechanical properties of TiAlSiN films[J]. Applied Mechanics and Materials, 2013, 421: 304-307.

[12] RUJISOMNAPA J, SURINPHONG S, WONGPANYA P. A comparative study of wear and oxidation behaviors of end mill coated by PVD coatings[J]. Advanced Materials Research, 2013, 785-786: 858-863.

[13] QIAO J W, WANG Y F, WANG R Q, et al. Tailoring microstructures and mechanical properties of AlCoCrFeNiTi0.3 high-entropy alloys by heat treatment[J]. Materials Science Forum, 2013, 745-746: 768-774.

[14] MILETIC A, PAN P, ŠJORIC B, et al. Microstructure and mechanical properties of nanostructured Ti-Al-Si-N coatings deposited by magnetron sputtering[J]. Surface and Coatings Technology, 2014, 241: 105-111.

[15] SATHIYAMOORTHI P, BASU J, KASHYAP S, et al. Thermal stability and grain boundary strengthening in ultrafine grained CoCrFeNi high entropy alloy composite[J]. Materials and Design, 2017, 134: 426-433.

[16] 顾俊峰, 邹 冀, 张 帆, 等. 高熵陶瓷材料研究进展[J]. 中国材料研究进展, 2019, 38(9): 855-865.
GU J F, ZOU J, ZHANG F, et al. Recent progress in high-entropy ceramic materials[J]. Materials China, 2019, 38(9): 855-865.

[17] WANG L, FU C, WU Y D, et al. Formation and toughening of metastable phases in TiZrHfAlNb medium entropy alloys [J]. Materials Science and Engineering A, 2019, 748: 441-452.

[18] CHEN L Q, LI W, LIU P, et al. Microstructure and mechanical properties of (AlCrTiZrV)N_x high-entropy alloy nitride films by reactive magnetron sputtering[J]. Vacuum, 2020, 181: 109 706.

[19] HAN J S, SU B, MENG J H, et al. Microstructure and composition evolution of a fused slurry silicide coating on MoNbTaTiW refractory high-entropy alloy in high-temperature oxidation environment[J]. Materials, 2020, 13(16): 3 592.

[20] WOO W, NAEEM M, JEONG J S, et al. Comparison of dislocation density, twin fault probability, and stacking fault

energy between CrCoNi and CrCoNiFe medium entropy alloys deformed at 293 and 140K[J]. Materials Science and Engineering A, 2020, 781: 139 224.

[21] BARSHILIA H C, GHOSH M, SHASHIDHARA, et al. Deposition and characterization of TiAlSiN nanocomposite coatings prepared by reactive pulsed direct current unbalanced magnetron sputtering[J]. Applied Surface Science, 2010, 256(21): 6 420-6 426.

[22] 李 芬, 朱 颖, 李刘合, 等. 磁控溅射技术及其发展[J]. 真空电子技术, 2011(3): 49-54.
LI F, ZHU Y, LI L H, et al. Review on magnetron sputtering technology and its development[J]. Vacuum Electronics, 2011(3): 49-54.

[23] ZHANG X, ZHOU Y W, GAO J B, et al. Effect of the filament discharge current on the microstructure and performance of plasma-enhanced magnetron sputtered TiN coatings [J]. Journal of Alloys and Compounds, 2017, 725: 877-883.

[24] MA Q S, LI L H, XU J B, et al. Effect of bias voltage on TiAlSiN nanocomposite coatings deposited by HiPIMS[J]. Applied Surface Science, 2017, 392: 826-833.

[25] 周子超, 张 豪, 张 雪, 等. 等离子体增强磁控溅射 CrSiN 涂层摩擦磨损行为[J]. 表面技术, 2020, 49(8): 185-191.
ZHOU Z C, ZHANG H, ZHANG X, et al. Friction and wear behavior of CrSiN coatings deposited by plasma enhanced magnetron sputtering [J]. Surface Technology, 2020, 49(8): 185-191.

[26] 张 勇, 陈明彪, 杨 潇, 等. 先进高熵合金技术[M]. 北京: 化学工业出版社, 2019.
ZHANG Y, CHEN M B, YANG X, et al. Advanced technology in high-entropy alloys[M]. Beijing: Chemical Industry Press, 2019.

[27] QIN X M, XU Y, SUN Y F, et al. Effect of process parameters on microstructure and mechanical properties of friction stir welded CoCrFeNi high entropy alloy[J]. Materials Science and Engineering: A, 2020, 782: 139 277.

[28] 贵宾华, 周 晖, 郑 军, 等. 偏压对 MPP 制备 AlTiSiN 纳米复合涂层结构及性能的影响[J]. 表面技术, 2020, 49(1): 228-236.
GUI B H, ZHOU H, ZHENG J, et al. Influence of bias voltage on microstructure and properties of AlTiSiN nanocomposite coatings prepared by MPP[J]. Surface Technology, 2020, 49(1): 228-236.

[29] ZHANG H, CHANG W J, LONG L, et al. Isothermal oxidation behavior of TiN coatings deposited by closed field unbalanced magnetron sputtering[J]. Materials Science and Engineering, 2019, 678: 012 158.

[编校:郑 霞]

(上接第 18 页)

[8] 冯冠文, 毕云杰, 王伟波, 等. 成形工艺对合金化锌基镀层微裂纹的影响研究[J]. 武汉工程职业技术学院学报, 2016, 28(3): 13-15.
FENG G W, BI Y J, WANG W B, et al. Analysis of zinc-coating micro-cracks after hot stamping [J]. Journal of Wuhan Engineering Institute, 2016, 28(3): 13-15.

[9] FAN D W, BRUNO C. State-of-the-knowledge on coating systems for hot stamped parts [J]. Steel Research International, 2012, 83(5): 412-433.

[10] WANG K, GUI Z X, LIU P X, et al. Cracking behavior of Al-Si coating on hot stamping boron steel sheet [J]. Procedia Engineering, 2014, 81: 1 713-1 718.

[11] ZHANG J, JIANG S M, ZHANG Q F, et al. Effect of temperature on microstructure and formability of Al-10wt%Si coating [J]. Journal of Iron and Steel Research, International, 2016, 23(3): 270-275.

[12] GHIOTTI A, BRUSCHI S, MEDDEA F. Comparison of tribological and wear performances of AlSi and Zn coatings in hot stamping of boron steel sheets [J]. Wear, 2015, 332-333: 810-821.

[13] 张 杰, 江社明, 张启富, 等. 热处理过程中纯锌镀层的组织转变和表面氧化[J]. 钢铁研究学报, 2014, 26(8): 42-46.
ZHANG J, JIANG S M, ZHANG Q F, et al. Microstructure transformation and surface oxidation of GI coating during heat treatment [J]. Journal of Iron and Steel Research, 2014, 26(8): 42-46.

[14] JANIK V, LAN Y J, BEENTJES P, et al. Zn diffusion and a-Fe (Zn) layer growth during annealing of Zn-coated B steel [J]. Metallurgical and Materials Transaction A, 2016, 47: 400-411.

[15] HYEON S H, JOONG C P, JONG S K, et al. Investigations on corrosion performance of galvanized 22MnB5 for hot press hardening under salt spray test: Test Proceedings of 9th International Conference on Zinc and Zinc Alloy Coated Steel Sheet & 2nd Asia-Pacific Galvanizing Conference[C]. Beijing: [s.n.], 2013: 726-729.

[编校:郑 霞]